A Statistical Investigation of the Influence of the Multi-Stage Hot-Drawing Process on the Mechanical Properties of Biodegradable Linear Aliphatic-Aromatic Co-Polyester Fibers

Basel Younes

Department of Textile Engineering, Faculty of Mechanical and Electrical Engineering, Damascus University, Damascus, P.O. Box 86, Syria

younesbasel@yahoo.co.uk

***Abstract*-This research investigates the influence of the hot-drawing process on the thermal shrinkage and mechanical properties of the bio-polymer fibers. As-spun fibers made of biodegradable linear aliphatic-aromatic co-polyester (LAAC) were drawn under a fractional factorial design as a function of hot-drawing conditions, the LAAC fibers were characterized and statistically modeled using appropriate experimental and statistical methods. According to the analysis, the most effective and significant parameters influencing the fiber mechanical properties are the drawing ratio and the drawing temperature. The significant factors affecting the thermal shrinkage are the total number of drawing stages (DS), the drawing temperature (DT), relaxing stage ratio (RS) and the plate temperature (PT). A new forecasting data source was achieved to optimize the hot drawing of as-spun aliphatic-aromatic co-polyesters (LAAC) fibers, and to specify the direction of increasing or decreasing of the significant process parameters. From the results and analysis, a combination of factor levels was designed for controlling the mechanical properties of the studied material using the regression equations obtained. With their elastical properties, the optimized aliphatic-aromatic co-polyester fibers with other biodegradable/bio-based materials could be used in agricultural, horticultural and other textile applications for sustainable development.**

Keywords- Biodegradable Polymer; Hot Drawing; Mechanical Properties; Thermal Shrinkage; Aliphatic-Aromatic Co-Polyester; Statistical Modeling; Bio-based Polymer Applications

I. INTRODUCTION

Biopolymers are non-toxic, recyclable and biodegradable polymers, their biodegradability is influenced by the chemical structure of the polymer chains, crystallinity, chain orientation and other morphological properties [1]. One of the novel biodegradable polymers is fully biodegradable petroleum aliphatic-aromatic co-polyester which is biodegradable under certain conditions, leaving no environmental footprint. The use of co-polyesters began in 1981 [2] when aliphatic-aromatic co-polyester fibers (LAAC) were developed, but they were not biodegradable fibers. AACs are made from petroleum and have stable physical and chemical properties, they have comparable cost to that of thermoplastic polymers. The commercial uses of biodegradable polyesters are paper coating, fibers, and refuse bags [3]. Aliphatic-aromatic co-polyesters are potential candidates for making staple fibers for various non-woven materials, particularly for expendable uses in medical [4-6] and agricultural applications [7-11]. As-spun fibers exhibit low tenacity and high elongation percentage, by post drawing the alignment of molecular chain and degree of crystallinity along the fiber axis can be improved. As-spun or un-oriented fibers should have a structure that can be drawn easily and be conductive to the formulation of extended chain and high orientation along the fiber axis. The main factors influencing the structure and the properties of drawn fibers are the as-spun fibers structure and the drawing conditions [12]. Drawing is an important stage in the case of the production process of synthetic fibers, it stabilizes the molecular structure and strengthens the yarn by improving the molecular orientation [13]. The drawing process results in highly oriented filaments with desired mechanical properties, pre-orientation and original structure of filaments [14]. All the as-spun fibers produced at different conditions could not be drawn to the same maximum draw ratio, each polymer has its natural draw ratio [15]. The drawability value of the as-spun fibers plays an important role in identifying the levels of the hot drawing parameters in the factorial experimental design theory. Structural properties affect strength, elongation, moisture absorption, absorption resistance and dye-ability; high orientation reduces molecular mobility and the dye-ability, which depends on the process parameters used and the polymer properties [16, 17]. Drawing tension is related to the stability of the process and the fiber texture as a function of drawing conditions. Drawing tension increases with the reduction of drawing temperature or with an increase of drawing ratio. With heating treatment and increasing the molecular mobility, the relaxation of internal stress can be achieved [18], heating treatment improves the ability of the fibers for drawing [19]. In technical terms, drawn fibers can be treated to improve the thermal stability even under controlled tension or in free state to eliminate the internal tensions by readjustment of intermolecular chemical links and of the crystallization degree [20].

After drawing, the relaxing process is necessary to obtain thermal stability in semi-crystalline fibers, there is some loss of orientation in the amorphous (non-crystalline) regions with a small amount of relaxing occurring [21]. Thermal properties

DOI: 10.5963/AMSA0304003

should be considered in that stage to monitor any change in the structure behavior. In scientific terms, if the effective glass transition temperature (Tg) is below the normal operation temperature, the crystallization will go to equilibrium only very slowly. In order to avoid this problem, it is necessary to heat the molded polymers (anneal) in an inert atmosphere at some temperature between (Tg) and melting temperature (Tm) in order to stabilize the polymer [22]. The extrusion temperature profile and polymer grade affect as-spun aliphatic–aromatic co-polyester fibers [23], melt spinning conditions affect the tensile properties of as-spun aliphatic-aromatic co-polyester fibers [24]. After drawing, the molecules are aligned in a more parallel arrangement and brought close together to be more crystalline and oriented [25]. The optimization and calibration are the most significant issues in any analytical methodology and quantization. The new software may help with the application of that technique for many applications and new product development [26, 27]. Statistical experimental design (SED) has the advantages of a one-step overall design in the development of process technology with known levels of the confidence model [28]. Statistical experimental design can help the engineering in designing the products and processes, developing the products and reducing the target value variation in processes.

The use of experimental design ideas is still limited because of inadequate education, familiarity with home-grown solutions (one factor per time), a lack of understanding of the statistical experimental design method and collaboration between academic and industrial fraternities, wrong ideas about experimentation requiring massive resources and proving expensive to execute, and poor attitude towards experimental design and the associated strategies [29]. With the elastic properties of bio-fibers, linear aliphatic-aromatic co-polyester fibers could be used in textile applications.

The main lines were used in this research to produce multifilament, single and simple untwisted yarns: for untwisted yarns, modelling the effect of the multi-stage hot drawing process on the thermal and mechanical properties of drawn linear (LAAC) aliphatic-aromatic co-polyester fibers were statistically investigated and characterized, it is generating new methods and analysis models saving the time and the cost of fiber production process. The achieved models help processing scientists and technologists in fibers industry to obtain the enhanced properties at suitable conditions related to final yarns cost, and to obtain environmentally friendly, economical and energy saving bio-fibers. The future work will deal with the twisting process and its interaction effect with the drawing process of studied fibers.

II. EXPERIMENTAL SECTION

A. Material

A fully biodegradable petroleum linear aromatic-aliphatic co-polyester, based on butandiol, adipic acid and terephthalic acid is supplied by Rodenburg Company, Netherlands, for use in this work. The polymer shape is spherical granule resin with diameter 3-5 mm and of density of 1.2 g/cc. LAAC can be melted in the temperatures range 110-115 ^{o}C. The material is referred to [30] as: 1,4-benzenedicarboxylic acid, polymer with 1,4-butanediol and hexanedioic acid. The supplier datasheet does not show the details related to copolymerization ratio, because it is a commercial sample. Owing to the low water solubility and high molecular weight of the polymer, it is unlikely to bio-accumulate [31], no eco-toxicity data were submitted [32] and no significant toxicological effect was observed [33].

B. Extrusion of As-Spun Fiber Sample by Melt Spinning

Fibers were extruded via melt-spinning using a Lab-spin machine, manufactured by Extrusion Systems Limited, UK. A special designed spinneret of 30 holes (0.4 mm diameter, l/d = 2) was used. Temperature profile and spinning conditions were selected based on statistical analysis and results of previous work [34-37]. The six heaters (zones) in the extrusion machine profile were 115, 120, 125, 130, 140 and 140 ^{o}C. The temperature of the feeding zone should be above 100 ^{o}C to prevent any moisture from forming. The molten polymer is forced through the spinneret as fine jets, with speed adjusted by the metering pump fixed at 12 rpm at 1000 psi (pre pump pressure). The air cooling quench speeds percentage was set at 73%. The spin finish (0.3 rpm) was diluted fivefold with water before use. Spin finish oil, VICKERS 1031, was used in the spinning and drawing processes. Godets and the winders were set at a speed of 50 m/min, and controlled independently by DC motors. The tension in the winder was controlled automatically to have good package build up and to avoid the high tension that affect the filament properties, the speeds were investigated by laser digital tachometer. The as-spun fibers drawability value will play an important role in identifying the levels of hot drawing parameters in the fraction factorial experimental design matrix.

C. Multi Stage Hot Drawing of As-Spun Fibers

For technical experimental reasons, the spinning and drawing processes were operated individually. In fact, the drawing process could be done at a higher speed than the melt spinning speed; therefore the drawing process is a separate operation from the spinning line [38]. After the as-spun fibers were extruded, hot drawing was carried out on an ESL (Extrusion System Limited), multi-stage draw frame (Fig. 1) which consists of four hot rollers (160 mm), three hot plates (495×30 mm) mounted between the rollers, a spin finish applicator and winder. Drawing took place at temperatures above Tg and in the phase of so-called rubber-like. The spun fibers have low glass transition (-33 to-30 ^{o}C) and low drawing temperatures could be used in a narrow temperature range. Fig. 2 shows an infrared image of a multi-stage hot drawing frame and one of the drawing rollers. In theory, solid-state (actual) draw ratio R and adjusted (machine) drawing ratio RD may be shown as:

DOI: 10.5963/AMSA0304003

$$[R = \frac{L_2}{L_1}(actual) \Leftrightarrow R_D = \frac{V_2}{V_1}(adjusted)] \quad (1)$$

where V1 = speed of the first drawing roll (m/min), V2 = speed of the second drawing roll (m/min), L1 = length of fiber before drawing, L2 = length of fiber after drawing.

The actual draw ratio is less than the nominal draw ratio because the draw line shrinks when tension is removed and yarn should not slip during drawing. In the case of non-linear viscoelastic behavior and necking effect, the velocity is neither steady nor uniform, and the kinematics problem of continuous drawing may be observed [18].

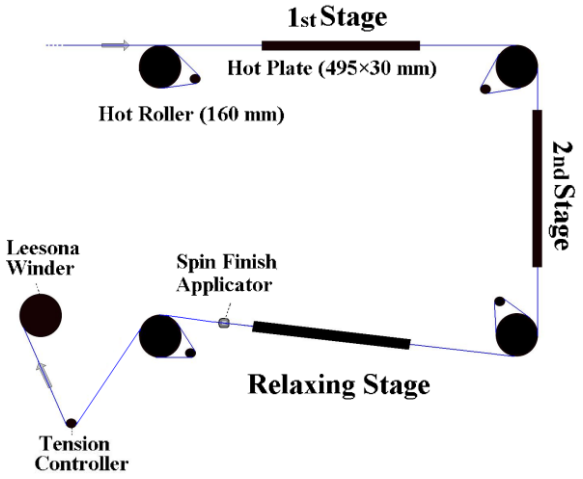

Fig. 1 Schematic diagram of the multi-stage drawing frame

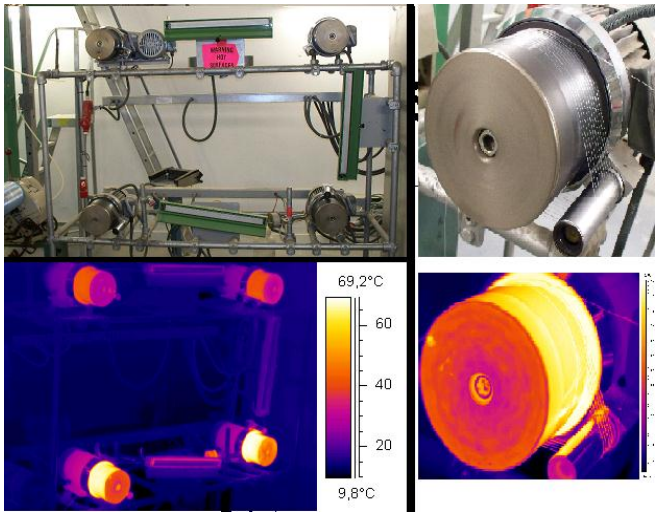

Fig. 2 Infrared image of multi-stage hot drawing frame and one of the drawing rollers
(Image colours correspond to the temperature scale on the right)

D. Differential Scanning Calorimetry (DSC)

A METTLER- TA Instrument DSC12E and METTLER –TOLEDO –TA89E System Software was used to determine the thermo-graphic behavior of LAAC fibers. The weight of the fiber specimen was from 5-10 mg in an aluminum pan with three decimal digits. In the case of nitrogen gas, the software offers the DSC graphs (heat flow/enthalpy curves) for the tested samples. Three replicates were scanned.

E. Mechanical Properties of LAAC Fibers

Tensile testing of fibers was carried out using an Instron tester (model 3345) connected to Instron Bluehill V 2.21 software at a temperature of 20 ±2 ^{o}C and relative humidity 65 ±5 %. The initial gauge length 20 mm was stretched at a constant cross head speed of 200 mm/min. Pre-tension of 0.005 N/tex was applied to the yarn to give a reproduce-able extension value; the samples were conditioned for 48 hours before testing. The reported results were the average values of five repeated measurements and the results were averaged to obtain a mean value. Samples were taken from different parts of a package and the elongation at break was measured as a percentage of the original length.

DOI: 10.5963/AMSA0304003

The stress-strain curve can be used to describe and classify the material qualitatively. Stress strain curve must be understood to decide the best strength and elongation for the yarn which is good for the weaving process [17]. When the fibers are tested until they break, they pass through many regions, including elastic region, yielding, strain hardening, necking and failure. It should be emphasized that the extent of each region in stress-strain space is material dependent, and not all materials exhibit all of the regions. At the yield point, the tensile filament starts to neck down and continues necking till the sample ruptures in the elastic region.

F. Thermal Shrinkage

Used fibers with their thermoplastic properties have created the need for the testing of shrinkage or extension of yarns and fabrics when subjected to heat. The thermal shrinkage test was carried out using the Testrite Thermal Shrinkage Oven, MK IV Shrinkage-Force from Testrite Ltd UK. The instrument (Fig. 3) comprises the heating chamber zone (250×110×80 mm), temperature controller, computer microprocessor, L.E.D readouts for results and the sliding carriage (which affords the means of mounting the test sample and presenting it to the heated zone), plus a load cell and free shrinkage attachment.

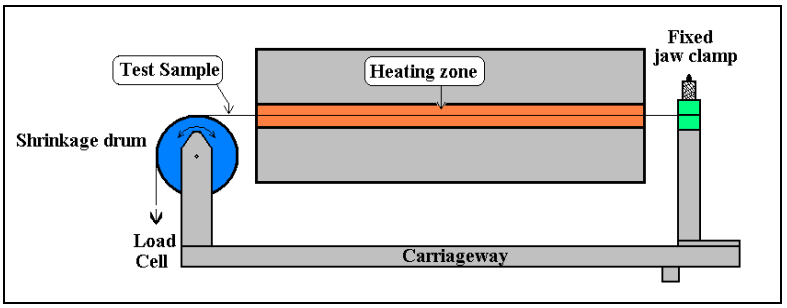

Fig. 3 Diagram of thermal shrinkage tester

The loaded threads carrier consisted of a jaw/clamp on one end and the free shrinkage drum with low torque potentiometer fitted to give the results on the other end. Using a load cell of 10 g and a shrinkage pot, the computer micro-processor determines the results shown on the front display panel, the movement expressed as a % of the sample length is related to shrinkage/extension under a constant tension during heating. Samples were heated for 2 minutes at 60 ^{o}C. The thermal shrinkage is calculated as 100 × (L0-L1)/L0, where L0 is the original sample length and L1 is the shrinkage/ extension sample length under a constant tension. The thermal stability is affected by influences of medium, sample weighting, temperature, time subjection to heat, count and structure of the sample, associated substances and evaluation parameter [20]. There is another effect from the fractional resistance between the fibers that transfers the forces between the fibers and raises the fraction.

III. RESULTS AND DISCUSSION

A. Factorial Experimental Design and Results

The aliphatic-aromatic co-polyester (LAACs) fibers were spun, hot drawn, characterized and analyzed under a fractional factorial design as a function of the process parameters using appropriate statistical methods to model the effect of the process parameters. A fraction factorial experimental design theory was used [39, 40]. Table 1 shows factor abbreviations and their levels for the hot drawing experiment. An L32 design matrix was used for the thirty-two screening trials in this experiment (Table 2), involving seven control parameters and two levels for each parameter, as shown in Table 1 designed using STATGRAPHICS software. As a function of hot-drawing conditions, a fractional factorial design with random order was used for the thirty-two screening trials in one block (L32; 27-2 = 25 = 32). The seven control parameters for the hot drawing experiments were as follows: drawing stages number (DS), drawing temperature (DT), total drawing ratio (DR), plat temperature (PT), spin finish (SF), relaxing stage ratio (RS) and relaxing temperature (RT) (see Table 1). The two levels of each parameter were separated as far apart as possible from each other.

The total drawing ratio (DR = DR1*DR2=V2/V1 *V3/V2 = V3/V1) has been used in the optimization, representing the ratio between the speed of the second roller (V3) of the second stage to the speed of the first roller of the first stage (V1). The speed of the second roller of the first stage equals the speed of the first roller of the second stage, V2. The draw ratio of the first stage (DR1:V2/V1) is larger than that of the second stage (DR2:V3/V2); the DR1 to DR2 ratio is 2 to 1. In two drawing stages, the same drawing temperature was applied for both the first and the second stages which decreased the number of interactions between the factors achieved, as a result of the ability of the software used, the relaxing stage helped in the deformability of the fiber by decreasing the internal stress inside the fiber. The relaxing stage helps in the deformability of the fiber. The mechanical properties and thermal shrinkage were measured, the values were averaged of three measurements for each sample represented by the random order number in the first column in the designed matrix Table 3. The means of measured data of the specimens have acceptable standard deviations which may be related to the draw frame setting based variation, the tension or slippage on the drawing roles or tension during the preparation of the sample for testing. An error could occur from one of two

DOI: 10.5963/AMSA0304003

assignable causes: variation resulting from changes in the independent factors, or random causes which are uncontrolled variation.

TABLE 1 FACTOR ABBREVIATIONS AND THEIR LEVELS FOR THE HOT DRAWING EXPERIMENT

Factor's abbreviation	Factor	Level	
		Low	High
A : DS	Total drawing stages number	1	2
B : DT	Drawing temperature (^{O}C)	40	60
C : DR	Total drawing ratio	3.5	5
D : PT	Plate temperature (^{O}C)	40	60
E : SF	Spin finish (rpm, 0.292 cc/rev)	0.2	0.4
F : RS	Relaxing stage ratio (%)	0.04	0.08
G : RT	Relaxing temperature (^{O}C)	30	50

TABLE 2 L32 EXPERIMENTAL DESIGN ARRAY FOR THE HOT DRAWING EXPERIMENT

Trial number	DS	DT	DR	PT	SF	RS	RT
1	1	60	5.0	40	1.5	0.04	60
2	2	40	5.0	40	3.0	0.04	60
3	2	60	3.5	60	1.5	0.04	60
4	1	60	5.0	60	1.5	0.04	40
5	2	60	5.0	40	1.5	0.08	40
6	2	60	3.5	60	3.0	0.04	60
7	2	40	3.5	60	3.0	0.08	40
8	1	60	3.5	60	3.0	0.08	40
9	2	40	5.0	60	3.0	0.04	40
10	2	40	3.5	60	1.5	0.08	40
11	1	60	3.5	60	1.5	0.08	40
12	2	60	3.5	40	3.0	0.04	40
13	2	40	5.0	60	1.5	0.04	40
14	1	60	3.5	40	3.0	0.08	60
15	1	40	3.5	40	3.0	0.04	40
16	2	40	3.5	40	1.5	0.08	60
17	1	60	3.5	40	1.5	0.08	60
18	1	40	3.5	40	1.5	0.04	40
19	2	60	5.0	40	3.0	0.08	40
20	1	40	3.5	60	3.0	0.04	60
21	1	40	3.5	60	1.5	0.04	60
22	2	40	5.0	40	1.5	0.04	60
23	2	60	5.0	60	1.5	0.08	60
24	2	60	5.0	60	3.0	0.08	60
25	1	60	5.0	40	3.0	0.04	60
26	1	40	5.0	40	1.5	0.08	40
27	1	40	5.0	40	3.0	0.08	40
28	1	60	5.0	60	3.0	0.04	40
29	1	40	5.0	60	3.0	0.08	60
30	1	40	5.0	60	1.5	0.08	60
31	2	60	3.5	40	1.5	0.04	40
32	2	40	3.5	40	3.0	0.08	60

TABLE 3 RESULTS FOR THE HOT DRAWING EXPERIMENTS

Trial Number	Thermal Shrinkage (%)	Tenacity (g/den)	Elongation at break (%)	Modulus (g/den)
1	11.9	1.0	91.67	1.66
2	14.6	1.3	81.94	1.90
3	14.9	0.6	222.92	0.48
4	11.5	1.0	79.17	1.69

DOI: 10.5963/AMSA0304003

5	14.0	1.1	84.72	1.64
6	14.1	0.6	193.75	0.45
7	14.0	0.7	183.33	0.81
8	09.8	0.7	200.00	0.47
9	14.2	1.3	84.72	1.92
10	14.0	0.8	220.83	0.45
11	10.3	0.8	183.33	0.45
12	14.9	0.8	183.33	0.48
13	14.3	1.0	56.94	1.55
14	10.2	1.0	241.67	0.50
15	13.0	0.7	195.83	0.74
16	13.8	0.6	175.00	0.47
17	11.3	0.8	222.92	0.44
18	13.5	0.8	195.83	0.54
19	14.1	1.1	95.83	1.63
20	13.1	0.7	212.50	0.51
21	13.0	0.8	187.50	0.48
22	14.4	0.9	62.50	2.01
23	14.0	1.1	86.11	1.67
24	12.5	0.9	77.78	1.71
25	12.4	1.1	91.67	1.47
26	12.4	1.0	70.83	1.56
27	13.7	1.1	75.00	1.64
28	11.7	1.1	100.00	1.64
29	13.1	1.1	77.78	1.69
30	13.3	1.2	76.39	2.16
31	15.4	0.7	210.42	0.49
32	14.5	0.8	193.75	0.45

To find the effect of hot drawing on the thermal properties of drawn fibers, Fig. 4 shows DSC curves for four selected samples produced with different hot drawing conditions for trials 4, 13, 23 and 30. No significant effect was reported in their thermal properties but the mechanical properties were better with the relaxation stage. A broad range of melting temperature (about 100-135 ℃) was observed for the fibers. According to the DSC results, the fiber did not melt completely below 120 ℃, as an optimum temperature window was found taking all factors into account. No appreciable changes of relative intensity of the peaks in the endotherm were observed in different samples for the same trial. In the drawing process, orientation is improved and molecules may be pulled out of the lamellar crystals and molecules in the amorphous regions are extended [15]. With heating, the chain will be flexible and will take the opportunity for a new and ordinary arrangement to be obtained at the achieved structure. In previous work, overall orientation and crystallinity were improved during hot drawing; molecules were pulled out of the lamellar crystals and molecules in the amorphous regions were extended [41, 42]. The mechanical properties depend on the drawing conditions and the original structure of un-drawn fiber which may be para-crystalline or amorphous [34-37, 43]. The fiber diameter affects the crystallization during drawing, the high value of fiber diameter helps the fiber to stay warm for longer periods of time. The stability will be less, with more internal strain, looking to get the original position and behaving like rubber.

The surface of the fiber and cross section shape were imaged using a scanning electron microscope (SEM). Fig. 5 shows an SEM photomicrograph of the surface and cross section of the fibers which have a round shape as expected from the used spinneret nozzles and the spinning method. Drawn fibers had a uniform circular cross section with acceptable uniform surface; the cross section of the fibers in the center could deform into a polygonal shape under pressure.

DOI: 10.5963/AMSA0304003

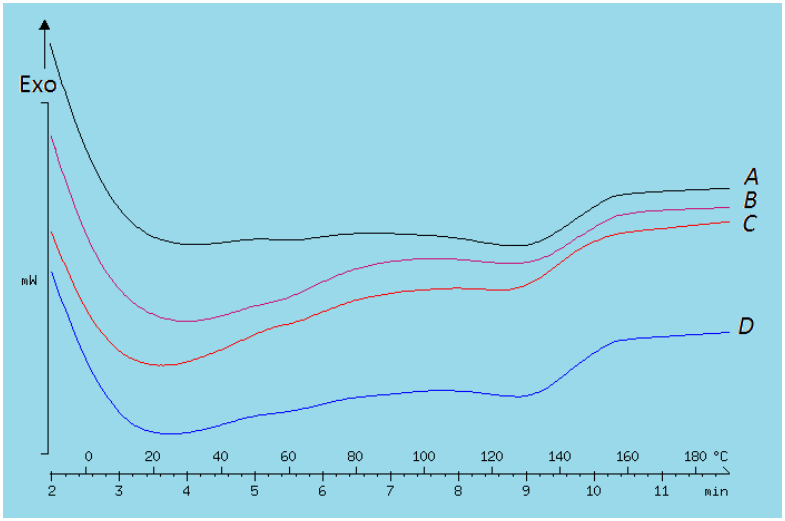

Fig. 4 DSC curves of hot drawn fibers
(A: trial 13, B: trial 23, C: trial 4 and D: trial 30)

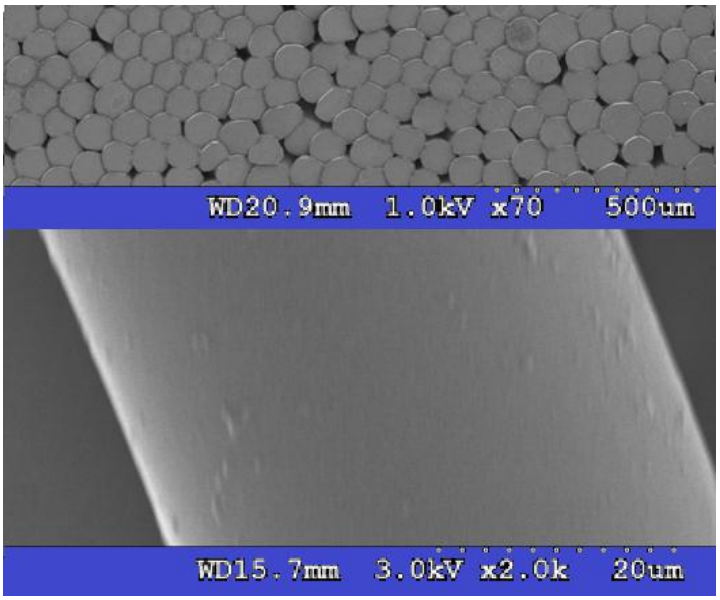

Fig. 5 SEM photomicrograph of the surface of the LAAC fiber and cross section

The major tools of statistical analysis include Pareto charts, effects and interaction plots, Daniel's plots, and Analysis of Variance (ANOVA). All of the statistical analysis and presented plots were constructed directly from the raw data using the computer software available STATOGRAPHICS and MINITAB. All of the statistical analyses and presented plots were constructed directly from the raw data using the available computer software. The results and statistical analysis helped in designing a combination of factor levels controlling the production processes of environmentally friendly biodegradable fiber. A combination of factor levels was designed for controlling the properties using the regression equations obtained by using Statographic Software.

B. Statistical Analysis of the Effects of the Factors and Their Interactions on the Responses

As a two-level experiment, the factor and interaction effects could be determined as the difference between the average responses at the low and high levels of hot drawing process parameters. A Pareto chart shows the significant arrangement of the factors and their interactions in decreasing order (y-axis) depending the significant effect (x-axis). Factors can have a positive (+) or negative (-) effect as presented by the colors pink and red respectively. The order of the significance of the factors is presented for each response and more interesting details will be described in the following statistical analysis to show the importance and the direct of the effect and the way in which the factors interact with each other.

Pareto charts (Fig. 6) for thermal shrinkage (a), tenacity (b), elongation at break (c) and modulus (d) show the significant arrangement of the factors and their interactions in decreasing order. A Pareto chart of the thermal shrinkage (a) is a useful tool for investigation of the extent to which a fiber has been heat stabilized. It shows that total drawing stages number (DS), the interactions (DS&DT, DR&RS and PT&RT), drawing temperature (DT), relaxing stage ratio (RS), the interactions (DS&DR

DOI: 10.5963/AMSA0304003

and DT&RS) and plate temperature (PT) are the most important factors affecting the thermal shrinkage properties of the fibers, followed by other factors and interactions. Determined factors would affect the tension and the internal stress affecting the orientation and the thermal shrinkage properties. In terms of the mechanical properties of drawn LAAC fibers, the Pareto chart for tenacity (b) shows that drawing ratio and the interactions PT&SF, DS&RT, DT&PT, DS&DR, DT&RS and SF&RS are the most important factors affecting the tenacity, followed by other factors and interactions.

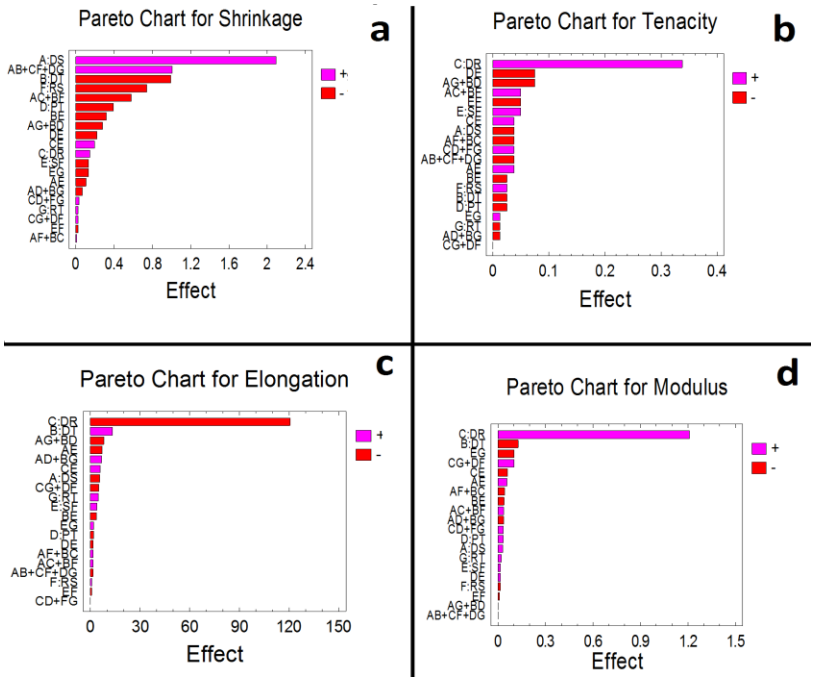

Fig. 6 Pareto chart for (a) thermal shrinkage, (b) tenacity, (c) elongation at break and (d) modulus

The Pareto chart for elongation at break (c) shows that total draw ratio (DR), drawing temperature (DT) and the interactions DS&RT, DT&PT and DS&SF are the most important factors affecting the elongation at break, followed by other factors and interactions. The Pareto chart for modulus (d) shows that total draw ratio (DR), drawing temperature (DT) and the interactions SF&RT, DR&RT and PT&RS are the most important factors affecting the modulus, followed by other factors and interactions. In the relaxation process and when the relaxing ratio increases, yarn speed decreases, cooling time increases and the thickness of the spin finish layer increases. This relationship could explain the interaction between process conditions and fiber structure; when a higher draw ratio is applied, the speed of the final roller will increase and the spin finish layer thickness on the fibers at constant spin finish pump speed will be affected, which could explain the interaction between the spin finish applicator speed and the draw ratio. The tension generated from applying a high drawing ratio with a lower relaxing ratio will create high internal stress in the biodegradable fiber structure and affect the shrinkage properties. The bio-polymer chains move in the direction of drawing to become oriented parallel to the fiber axis. As a second order transition is obtained with high relaxing stage ratio and with lower temperature in the relaxing stage, the chains lose their freedom and elasticity and so become fixed. The main effects and interaction plots of the statistical analysis of the effects are other statistical-based techniques which could give an additional idea about the effects of factors on studied responses. The effect line determines the effect of the factors from the length and the slope of the line between the two levels. The longer the effect line the more significant the factor effect. The direction of the effect is determined by the slope of the line: a positive effect is obtained when the line increases from the left to the right and vice versa. The effect of factors on thermal shrinkage and mechanical properties between the average responses of the low and high level of the factors was obtained using the design matrix, and is presented in Figs. 7-10 (a). For example, tenacity increases either by increasing the draw ratio or by decreasing the drawing temperature. All the interactions could be simulated, as the plot shows the existence or otherwise of each two factor interaction, as coded in Table 1. To determine the form of the interaction between each two factors together and how the direction of change of the interacting factors influences the change on the fiber properties, an interaction plot is needed (Figs. 7-10 (b, c and d)). All the interactions could be simulated, as the plots show the existence or otherwise of the interaction of each of the two factors. The interaction between the number of drawing stages and drawing temperature is presented as AB:DS&DT on the plot (Fig. 7 (b)). The first factor (A:DS) is presented on the X-axis from low level to high level, while the second factor (B:DT) is shown as two different lines, one for low level coded as (-) and another for high level coded as (+). When the high level of the number of drawing stages was paired with the high level of drawing temperature, the maximum thermal shrinkage was obtained; the nonparallel lines confirm the presence of an intersection. From the main effects plot for the thermal shrinkage, the main effects of the total number of drawing stages, drawing temperature, relaxing stage ratio and plate temperature were more pronounced than those of the other factors, total draw ratio, spin finish application and relaxing temperature, as their lines were longer and their slopes sharper than those of the other factors. The interactions DS&DT, DR&RS, PT&RT, DS&DR, DT&RS and DT&SF will be

DOI: 10.5963/AMSA0304003

further investigated using ANOVA analysis. Thermal shrinkage increased either by increasing the number of drawing stages and drawing ratio, or by using the lower level of other factors which affected negatively the thermal shrinkage. The effects and interaction plots for tenacity (Fig. 8) show that total draw ratio and the interactions (PT&SF, DS&RT, DT&PT, DS&DR, DT&RS and SF&RS) were the most important factors. From main effects and interaction plots for elongation at break (Fig. 9), total draw ratio, drawing temperature, DS&RT, DT&PT and DS&SF were the factors affecting the elongation at break. The effects and interaction plots for the modulus (Fig. 10) show that total draw ratio, drawing temperature and the interactions SF&RT, DR&RT and PT&RS affect the modulus. In the relaxation stage, the chains could return to their random arrangement, depending on the total draw ratio.

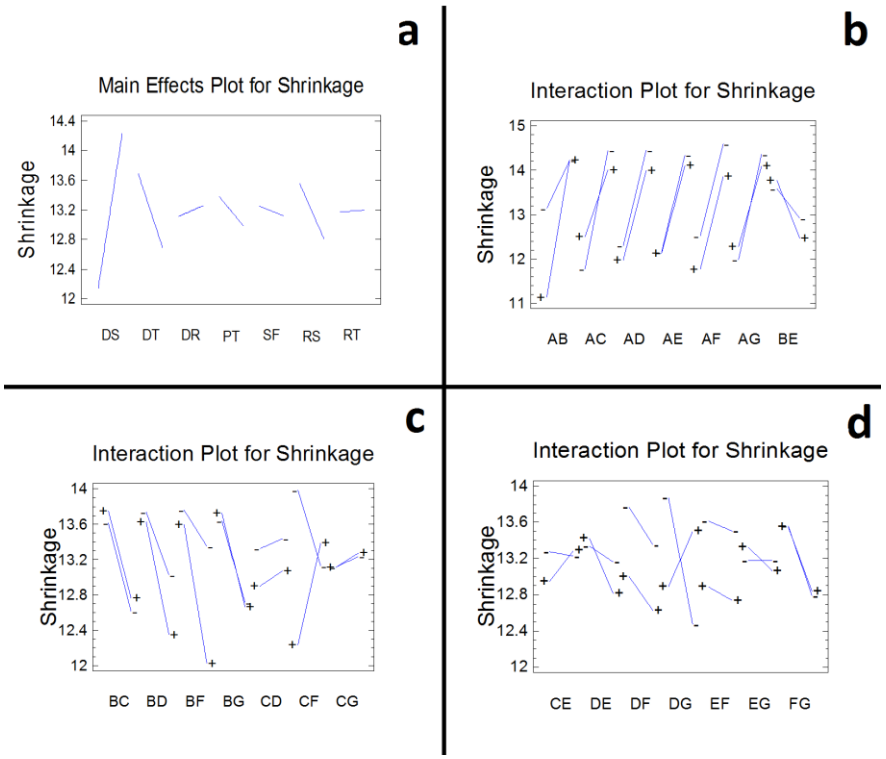

Fig. 7 Main effect plots and interaction plots for the thermal shrinkage

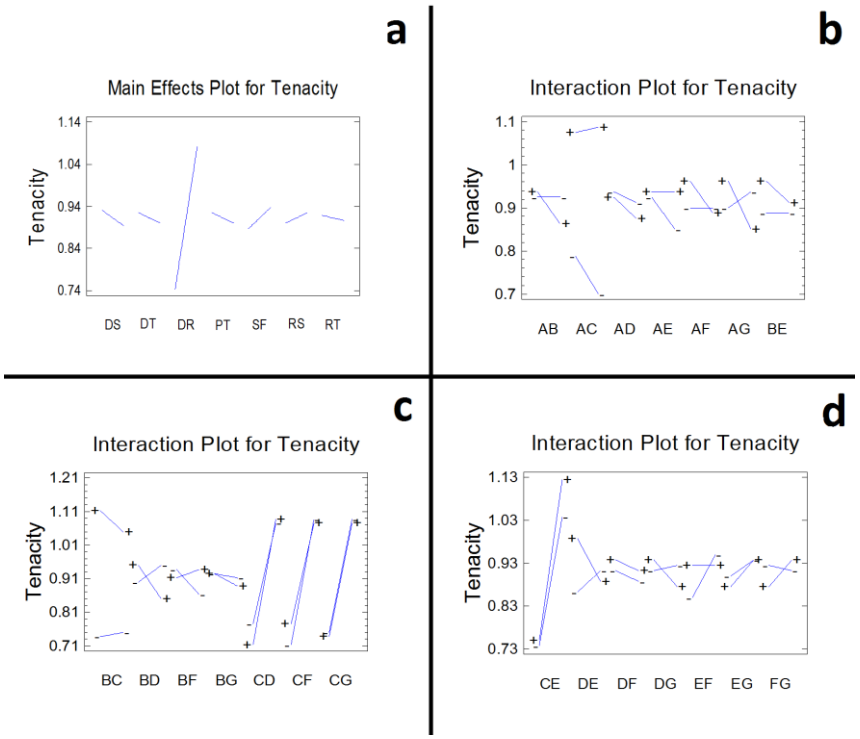

Fig. 8 Main effect plots and interaction plots for the tenacity

DOI: 10.5963/AMSA0304003

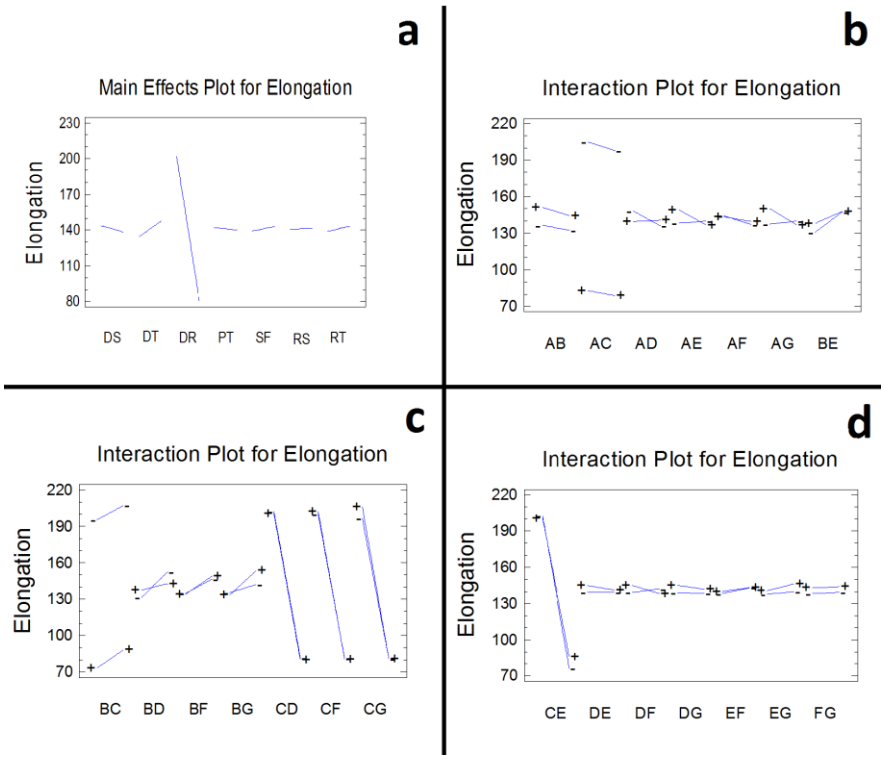

Fig. 9 Main effect plots and interaction plots for the elongation at break

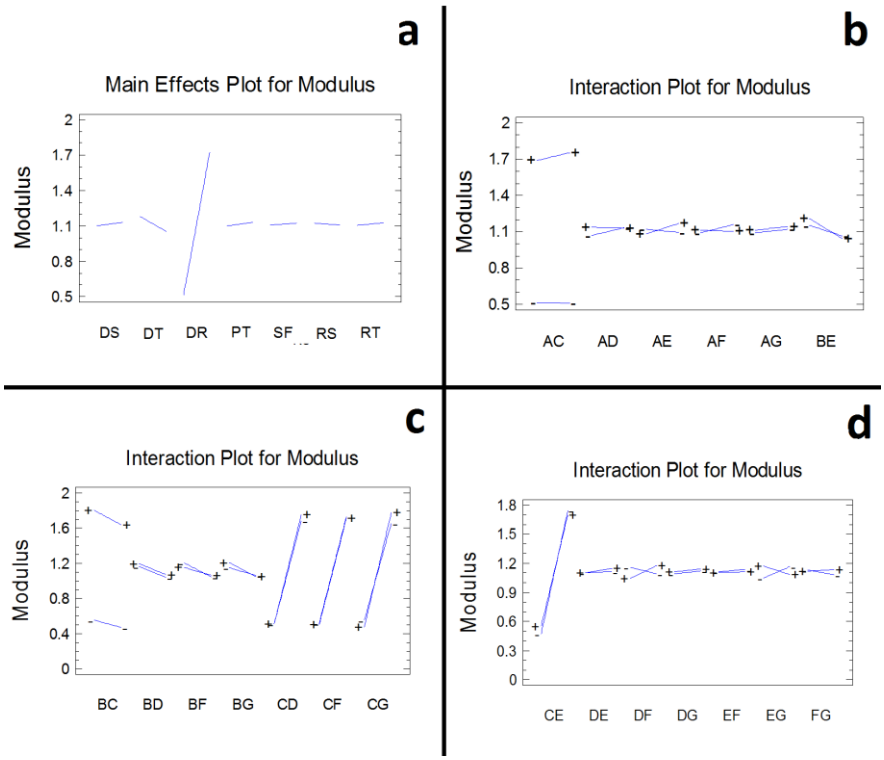

Fig, 10 Main effect plots and interaction plots for the modulus

A STATGRAPHICS program is used to calculate statistical standardized and percentage order factors and their interactions values; they are then plotted on X and Y axes respectively to generate a normal probability plot or a Daniel's plot (Fig. 11). This technique helps in the separation process of factors into important/unimportant categories, and gives more details concerning whether the effect of the factor is positive or negative [27]. The straight line represents the empirical principle in the middle of the range, the significant effect for both positive and negative effect could be reflected in deviation of the data points from the straight line. The further the deviation, the greater the statistical significance. If responses follow a normal distribution pattern, that means there are no statistically significant factor effects in the experiment. Fig. 11 displays the normal

DOI: 10.5963/AMSA0304003

probability plot of the responses estimated, and illustrates further details about the normal distribution for the data. Fig. 11 (a) displays the normal probability plot for the thermal shrinkage. In the relaxation process, when the relaxing stage ratio increases, the yarn speed decreases, the cooling time increases and the thickness of the spin finish layer will be increased. That relationship could help in understanding the interaction between process conditions and fiber structure. Some interactions between factors could be related to the fractional design; these results were analyzed by ANOVA. The positive effects from the total number of drawing stages (DS) and the interactions DS&DT, DR&RS and PT&RT are prominent. Drawing temperature (DT), relaxing stage ratio (RS) and the interactions DS&DR and DT&RS had a negative effect on thermal shrinkage. In terms of mechanical properties, draw ratio had a negative effect on elongation at break and a positive effect on tenacity and modulus. Draw temperature had either a positive effect on elongation at break or a negative effect on tenacity and modulus. Other factors and interactions had a less significant effect on mechanical properties. With one stage, the tension will be very high, and the spin finish plays an important role in the filament slippage on the last roller after applied spin finish, in addition to the spin finish in the as-spun samples. Increasing the draw ratio or decreasing the drawing temperature plays an important role in stretching the chain inside the fibers, resulting in an improvement in the mechanical properties of the fiber. The effects from the interaction between draw stage and spin finish could be related to the practical relationship between the tension and the oily roller surface on the last roller in the relaxing stage ratio which caused some slippage.

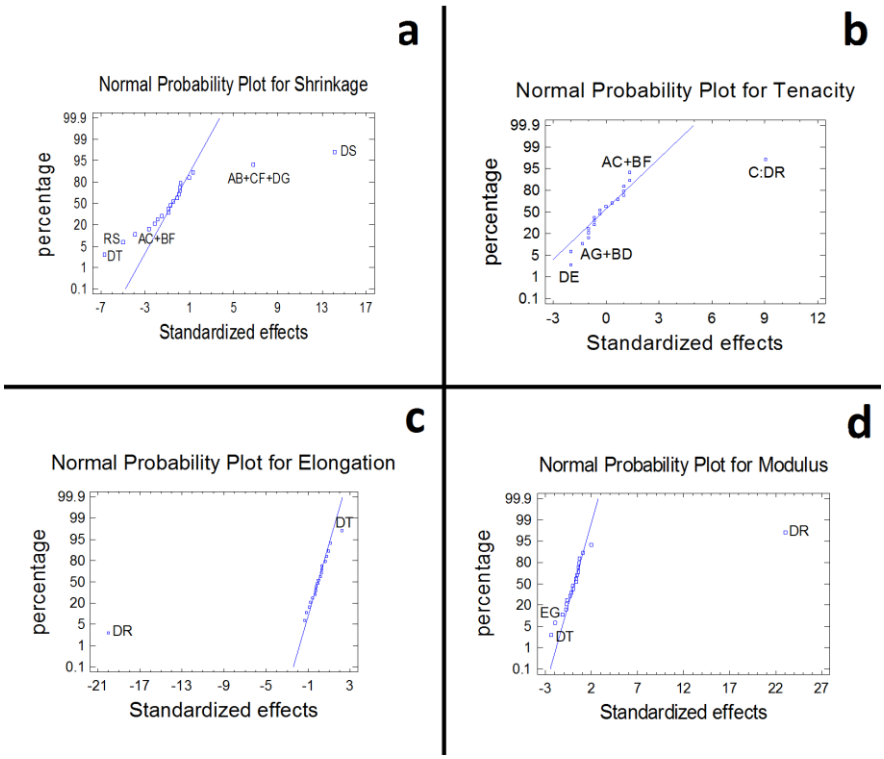

Fig. 11 Normal Probability Plot for (a) thermal shrinkage, (b) tenacity, (c) elongation at break and (d) modulus

C. Analysis of Variance (ANOVA)

In order to determine the factor effects in terms of statistical significance, analysis of variance (ANOVA) of the obtained data is needed. The ANOVA method is a mathematical method based on statistical data by which the response data to the error data can be compared and the significant effect of the independent factors or from their interaction can also be assessed. ANOVA depends on the F test, the F-ratio being obtained from statistical F Tables at the appropriate level α =0.05 [39]. If the F value is greater than the critical F value, F= 4.84 in used design, its factor has a significant effect on the response. After calculating the F value, the P value is determined using the graphic method (P ≡ α-significance level) and can be obtained from most modern statistical analysis programs. A probability or P-value used in ANOVA provides quantitative and objective criteria for judging the statistical significance of the effects. Each factor has a P-value less than 0.05, indicating that the factor is significantly different from zero at the 95.0% confidence level. The ANOVA results are listed in Table 4. The significance of the studied factors affecting the thermal shrinkage will then be the total number of drawing stages (DS)> the interactions DS&DT, DR&RS and PT&RT > drawing temperature (DT)> relaxing stage ratio (RS) > the interactions DS&DR and DT&RS > plate temperature (PT). The interaction DT&SF was on the borderline of significance effect. There were no significant effects of the other interactions within the factor range in the experiments. The ANOVA analysis for mechanical properties shows that the draw ratio had a significant effect on tenacity, elongation at break and modulus. Drawing temperature had a significant effect on elongation at break and modulus, as it affected the internal structure of the fibers. According to the statistical analysis, the most effective and significant parameters on mechanical properties are the drawing ratio and the drawing temperature. Other factors and interactions had their effect, but they were limited and less significant; they were

DOI: 10.5963/AMSA0304003

overcome by the significance of the drawing ratio and drawing temperature. An error could result from either assignable causes that represent variation resulting from changes in the independent factors, or random causes that signify uncontrolled variation.

TABLE 4 THE ANALYSIS OF VARIANCE (ANOVA) RESULTS FROM OF THE DATA IDENTIFYING THE STATISTICAL SIGNIFICANCE OF EACH FACTOR FOR THERMAL SHRINKAGE, TENACITY, ELONGATION AT BREAK AND MODULUS

Source	P-Value			
	Thermal Shrinkage	Tenacity	Elongation at break	Modulus
DS	0.0000	0.3365	0.3801	0.5864
DT	0.0000	0.5166	0.0480	0.0354
DR	0.3524	0.0000	0.0000	0.0000
PT	0.0222	0.5166	0.7627	0.5554
SF	0.3943	0.2072	0.5349	0.7535
RS	0.0004	0.5166	0.8826	0.7535
RT	0.9015	0.7439	0.4490	0.6844
DS&DT DR&RS PT&RT	0.0000	0.3365	0.8166	0.9907
DS&DR DT&RS	0.0024	0.2072	0.8059	0.5107
DS&PT DT&RT	0.6514	0.7439	0.2883	0.5107
DS&SF	0.4879	0.3365	0.2710	0.3010
DS&RS DT&DR	0.9671	0.3365	0.7842	0.4682
DS&RT DT&PT	0.0840	0.0696	0.2099	0.9907
DT&SF	0.0543	0.5166	0.5716	0.4821
DR&PT RS&RT	0.8367	0.3365	0.9945	0.5403
DR&SF	0.2173	0.3365	0.3659	0.2813
DR&RT PT&RS	0.9015	1.0000	0.4332	0.0748
PT&SF	0.1675	0.0696	0.7735	0.7535
SF&RS	0.9015	0.2072	0.9050	0.8613
SF&RT	0.3943	0.7439	0.7627	0.0748

The geometric result of plotting a response variable was as a function of two factors; the interaction appeared with the surface twist (Fig. 12). The estimated response surface was based on the assumed regression model. The estimated response surfaces of thermal shrinkage were used to determine the direction and the significance of the interactions, as shown in Fig. 12 (a). In order to determine the direction of the interactions DS&DT, DR&RS and PT&RT, the geometric result of plotting a response variable was required. There was a twist which confirmed the interaction between the total number of drawing stages and drawing temperature. As the surface was flat with no twist found in the surface DR&RS and PT&RT, their determined effects were not significant. This corresponds with the previous statistical analysis results of the interaction plot and ANOVA derived from the experimental data. There was a significant interaction between the number of drawing stages and drawing ratio as there was no twist in the estimated response surface for the insignificant interaction DT&RS. The interaction between DT&SF was borderline and noted twist was found in the surface.

DOI: 10.5963/AMSA0304003

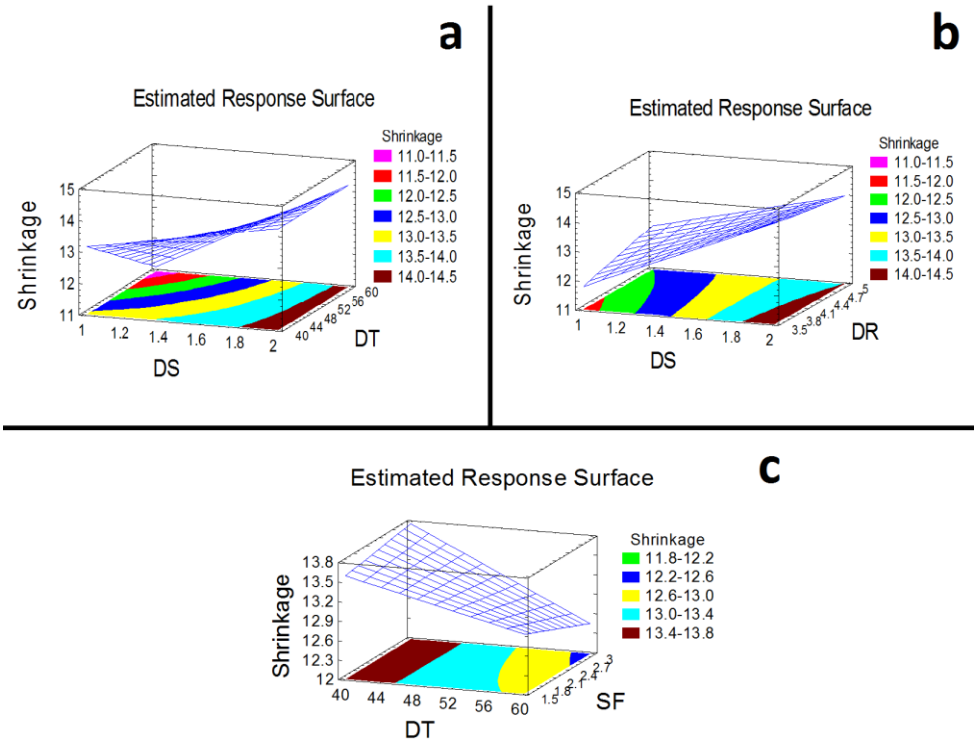

Fig. 12 The estimated response surface for the interactions (DS&DT, DS&DR and DT&SF) for thermal shrinkage

D. The Regression Equation and Estimation Results

Based on the analysis of the fraction factorial experimental design (L32) results, simplified forecasting models based on statistical analysis for studied factors and their interactions were fitted by the regression equations for thermal shrinkage, tenacity, elongation at break and modulus; these have been fitted to the experimental data. Enhanced regression equations forecast the fiber properties in order to achieve the most satisfactory properties in the final desired fiber for different applications. The regression equations in terms of the previous coded values (Table 1) are given as follows:

[Thermal shrinkage = 11.1573 + 2.40625*DS - 0.152812*DT + 0.704167*DR + 0.0145833*PT + 1.65972*SF - 17.6563*RS + 0.0575*RT + 0.100625*DS*DT - 0.775*DS*DR - 0.006875*DS*PT - 0.141667*DS*SF + 0.3125*DS*RS - 0.028125*DS*RT - 0.02125*DT*SF + 0.00208333*DR*PT + 0.172222*DR*SF + 0.00125*DR*RT - 0.0145833*PT*SF - 0.625*SF*RS - 0.00875*SF*RT] (2)

[Tenacity = -0.4875 + 0.304167*DS + 0.008125*DT - 0.075*DR + 0.00125*PT + 0.208333*SF + 7.1875*RS + 0.00875*RT - 0.00375*DS*DT + 0.0666667*DS*DR - 0.00125*DS*PT + 0.05*DS*SF - 1.875*DS*RS - 0.0075*DS*RT - 0.00166667*DT*SF + 0.0025*DR*PT + 0.0333333*DR*SF + 0.0*DR*RT - 0.005*PT*SF - 1.66667*SF*RS + 0.000833333*SF*RT] (3)

[Elongation at break = 361.045 + 15.4508*DS + 1.413*DT - 78.3267*DR - 0.823583*PT + 7.97278*SF - 48.9375*RS + 2.551*RT - 0.14325*DS*DT + 2.02333*DS*DR + 0.67275*DS*PT - 9.31833*DS*SF + 84.625*DS*RS - 0.803*DS*RT - 0.234417*DT*SF - 0.00283333*DR*PT + 5.05444*DR*SF - 0.327*DR*RT - 0.118583*PT*SF - 24.5417*SF*RS + 0.124417*SF*RT] (4)

[Modulus = -1.61469 - 0.040625*DS - 0.00046875*DT + 0.39875*DR - 0.00497917*PT + 0.555139*SF + 3.23438*RS - 0.0125625*RT - 0.0000625*DS*DT + 0.0475*DS*DR - 0.0035625*DS*PT + 0.0758333*DS*SF - 1.96875*DS*RS - 0.0000625*DS*RT - 0.00254167*DT*SF + 0.00220833*DR*PT - 0.0527778*DR*SF + 0.006875*DR*RT + 0.001125*PT*SF - 0.3125*SF*RS - 0.006875*SF*RT] (5)

The models evaluated the significance effect of each independent variable to a predicted response depending on the coefficient constant for the linear effects of independent factors and the coefficient constant for the effects of interaction, depending on the coefficient constant for the offset term. Fig. 13 shows the experimental results observed, and the calculated fitted results plot for thermal shrinkage (a), tenacity (b), elongation at break (c), and modulus (d). The experimental results observed were plotted on the Y axis and data for calculated fitted results generated using the last fitted model were plotted on the X axis for each trial. While the point estimate gives the best possible prediction, the prediction could be not perfect.

DOI: 10.5963/AMSA0304003

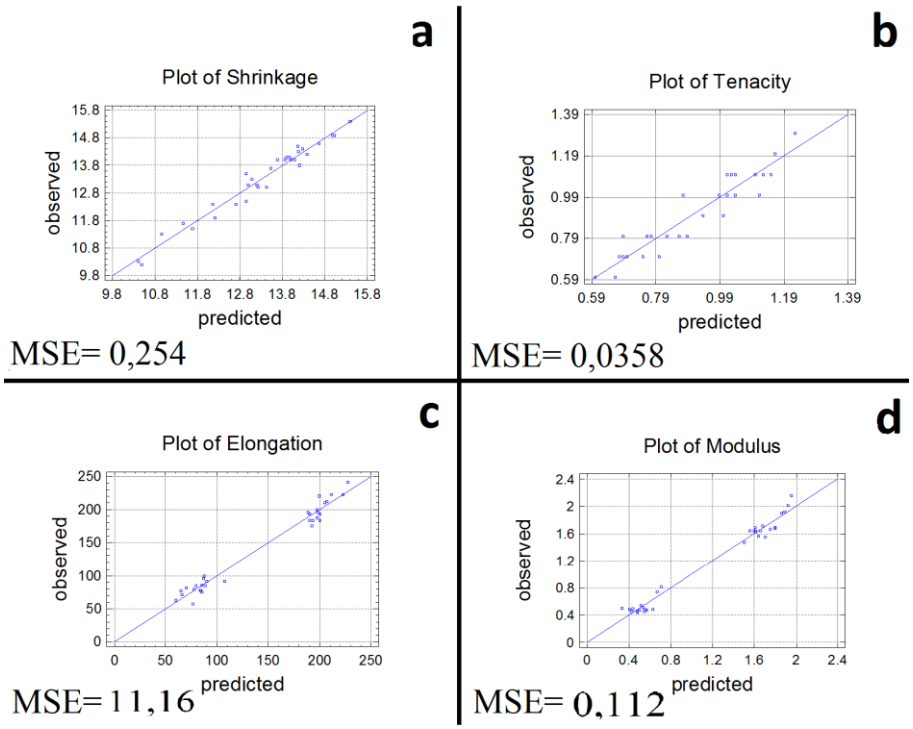

Fig. 13 Experimental observed results and calculated fitted results plot for (a) thermal shrinkage, (b) tenacity, (c) elongation at break and (d) modulus

The error in prediction could be incorporated by using interval estimates rather than point estimates or further regression. Theoretically, the software obtains the standard deviation of the mean values and then estimates the range of values which would encompass the predicted and observed values. A new name is assigned to the standard deviation of the means, which is the standard error. Standard deviation reflects the variability of individual data points, and the standard error is the variability of calculated and predicted values of the responses. By itself, the Model Standard Error (MSE) is used in constructing confidence intervals (CIs), which indicate a range of values within which the "true" value lies. It shows how accurate the estimates of the population values actually are. Both statistical significance testing and CIs are useful because they assist the reader in determining the meaning of the results. MSE is calculated by the software used; the intervals bound the sampling error in the estimates and judge precisely the mean of each response. The predictive models gave useful results if the draw frame setting based variation, the tension or slippage on the drawing roles and some tension during the preparation of the sample for testing were controlled and taken into account. To establish how accurate the estimate is, their Model Standard Error (MSE) values presented in Fig. 13 indicate the dispersion of predicted and observed values around the theoretical fitted line generated using the fitted model for each trial. The pattern of estimated responses was based on the assumed model derived from the experimental observations. Table 5 shows the combination of factor levels over the indicated region which maximize and minimize the responses, which are thermal shrinkage, tenacity, elongation at break and modulus. To explain the interaction effect between the analyzed factors, some facts should be considered from the scientific point of view: when a higher draw ratio is applied, the speed of the final roller will increase which could explain the effect of the interaction between the spin finish and the draw ratio on cooling time, the internal stress of fibers is decreased in the relaxing stage to allow the new form to stabilize by re-crystallization.

TABLE 5 THE COMBINATIONS OF FACTOR LEVELS FOR THE EFFECT OF MULTI-STAGE HOT DRAWING ON THE PROPERTIES OF LINEAR ALIPHATIC-AROMATIC CO-POLYESTER FIBERS FOR THERMAL SHRINKAGE, TENACITY, ELONGATION AT BREAK AND MODULUS

Response	Optimum model	The combination of factor levels (↓: Low Level, ↑: High Level)						
		DS	DT	DR	PT	SF	RS	RT
Thermal Shrinkage (%)	Maximum	↑	↑	↓	↓	↓	↓	↓
	Minimum	↓	↑	↓	↑	↑	↑	↓
Tenacity (g/den)	Maximum	↑	↓	↑	↓	↑	↓	↓
	Minimum	↑	↑	↓	↑	↓	↓	↑
Elongation at break (%)	Maximum	↓	↑	↓	↓	↑	↓	↑
	Minimum	↑	↓	↑	↓	↓	↓	↑
Modulus (g/den)	Maximum	↓	↓	↑	↑	↓	↑	↑
	Minimum	↓	↑	↓	↓	↑	↓	↑

DOI: 10.5963/AMSA0304003

In conclusion and according to the analyses, the most effective and significant parameters influencing the fiber thermal shrinkage and mechanical properties are the drawing ratio and the drawing temperature. Other effects are overcome by the significance of the drawing ratio and drawing temperature. Mechanical properties of used biodegradable fibers are affected positively by drawing ratio and plat temperature, and negatively by drawing temperature, the interaction between drawing stage and relaxing temperature, relaxing temperature and the interaction between draw ratio and spin finish. By increasing the relaxing temperature, increasing the molecular mobility and decreasing of internal stress could be achieved. Drawing tension is related to the stability of drawing conditions. It was increased with a reduction of drawing temperature or increase of drawing ratio. In other words, increasing the number of drawing stages and plate temperature decreased the degree of crystallographic order of the biodegradable fibers, even if they have no significant effects. Alternatively, when a higher draw ratio is applied, the speed of the final roller will increase and the spin finish layer thickness on the fibers at constant spin finish pump speed will be decreased, which could explain the interaction between the spin finish and the draw ratio increasing, in terms of cooling time effect. The possible mechanism of the effect of the spin-finish application on the crystallographic order is a heat transfer and cooling effect in the number of drawing stages caused by friction or slippage (stick-slip) in the drawing and relaxing stage. Drawing tension of biodegradable fibers is related to the stability of drawing conditions: it is increased with the reduction of drawing temperature or increasing of drawing ratio.

IV. CONCLUSIONS

As-spun, biodegradable, linear aliphatic-aromatic co-polyester (LAAC) fibers were drawn at different multi-stage hot drawing process conditions. The drawing and mechanical properties of the LAAC fibers were characterized and statistically modelled. The statistical models covered the number of drawing stages, drawing temperature, total drawing ratio, plate temperature, spin finish application, relaxing stage ratio, relaxing temperature and their interactions. The models specified the combinations of their levels for enhancing properties.

There are three noted factors affecting the tension and the internal structure, and then the thermal shrinkage; these are the number of drawing stages, drawing temperature and relaxing stage ratio. Plate temperature and the interactions DS&DT, DR&RS and PT&RT have a notable effect on the thermal shrinkage. Some interactions between factors could be related to the fractional design, as mentioned before. The number of drawing stages and relaxation stages and their interactions with temperature would affect the internal tension of the fiber chains which creates strain inside the fiber structure. As the relaxation stage ratio increases, the yarn speed decreases and more time is available for the relaxation process. The strain affects the freedom and the flexibility of the molecules, which in turn affect the shrinkage properties. Mechanical properties of used fibers are significantly affected by draw ratio and draw temperature, the most effective and significant parameters. Other factors and interactions have their effects, but they are limited and less significant as they are covered by the governing factors which are drawing ratio and temperature. Increasing the draw ratio or decreasing drawing temperature plays an important role in stretching the chain inside the fibers, resulting in an improvement in the fiber's internal structure. With one stage, the tension will be very high and the spin finish plays an important role in the filament slippage on the last roller after the applied spin finish, in addition to the spin finish in the as-spun samples. In the relaxation process, when the relaxing stage ratio increases, the yarn speed decreases, the cooling time increases and the spin finish layer's thickness will be increased; the cooling action consequently affects the crystal structure arrangement. With the elastic properties of bio-fibers, linear aliphatic-aromatic co-polyester fibers could be used in agricultural, horticultural and more non-traditional textile applications. The regression equations achieved form a part in a forecasting program designed to optimize the drawing process of selected as-spun fibers, which will be published in future for the production process. The future work will deal with the twisting process and its interaction effect with the drawing process of studied fibers.

ACKNOWLEDGMENTS

The author is indebted to Dr. Alex Fotheringham in the School of Textiles and Design/Heriot-Watt University for his greatly valued support and supervision in the analyzing stage in the extrusion lab and to Mr. James McVee in the School of Textiles and Design/Heriot-Watt University for his greatly appreciated technical support on testing equipment. The author is also indebted to the Textiles department/ FMEE/Damascus University for the research support.

REFERENCES

[1] H.C. Ki and O.O. Park, "Synthesis, characterization and biodegradability of the biodegradable aliphatic-aromatic random copolyesters," *Polymer*, vol. 42, pp. 1849-1861, 2001.

[2] P. Bajaj, "Aliphatic-Aromatic Copolyester Fibers, Part I. Effect of Bisphenols on Structure and Mechanical Properties," *Textile Research Journal*, vol. 51, pp. 696-703, 1981.

[3] Q. Fang and M.A. Hanna, "Preparation and Characterization of Biodegradable Copolyester–Starch Based Foams," *Bio-resource Technology*, vol. 78, pp. 115-122, 2001.

[4] M. Renke-Gluszko and M.E. Fray, "The effect of simulated body fluid on the mechanical properties of multiblock poly(aliphatic/aromatic-ester) copolymers," *Biomaterials*, vol. 25, pp. 5191-5198, 2004.

DOI: 10.5963/AMSA0304003

[5] P. Prowans, M.E. Fray, and J. Slonecki, "Biocompatibility studies of new multiblock poly(ester-ester)s composed of poly(butylene terephthalate) and dimerized fatty acid," *Biomaterials*, vol. 23, pp. 2973-2978, 2002.

[6] B.L. Seala, T.C. Oterob, and A. Panitch, "Polymeric biomaterials for tissue and organ regeneration," *Materials Science and Engineering*, vol. 34, pp. 147-230, 2001.

[7] K. Twarowska-Schmidt, "Evaluation of the Suitability of Some Biodegradable Polymers for the Forming of Fibers," *Fibers & Textiles in Eastern Europe*, vol. 12, pp. 15-18, 2004.

[8] L. Fumin, W.A. Haile, M.E. Tincher, and W.S. Harris, "Bio-Degradable Copolyester Nonwoven Fabric," European Patent EP1330350, 2003.

[9] J.H. Wang and H. Aimin, "Biodegradable Aliphatic-Aromatic Copolyester for use in Nonwoven Webs," 2008.

[10] F. LU, W. Ahaile, M. Etincher, and S.H. Wiley, "Bio-degradable Copolyester Nonwoven Fabric," 2002.

[11] K. Twarowska-Schmidt and M. Ratajska, "Biodegradability of Non-Wovens Made of Aliphatic-Aromatic Polyester," *FIBERS & TEXTILES in Eastern Europe*, vol. 13, pp. 71-74, 2005.

[12] M. Karaman and C. Batur, "Proceeding of American control conference Philadelphia," *Draw Response Control for Polymer Fiber Spinning Process*, 1998.

[13] P. Lord, Hand Book of Yarn Production: Technology Science and Economics, The Textile Institute & CRC & WP England, 2003.

[14] L. Hes and P. Ursiny, Yarn Texturizing Technology, EEC Comett program & Eurotex Portugal, 1994.

[15] C. Andreoli and F. Freti, Man-made fibers, ACIMIT: Italy 2004.

[16] S.J. Kadolph and A.L. Langford, Textiles Pearson Education Inc, USA, 2002.

[17] H. Brody, Synthetic fiber materials, Longman group UK limited London, 1994.

[18] A. Ziabicki, Fundamental of Fiber Formation, John Wiley &Sons: London, 1976.

[19] H.F. Giles, J.R. Wagner and E.M. Mount, "Extrusion: the Definition Processing Guide and Hand Book," William Andrew Inc: Norwich, 2005.

[20] J.W.S. Hearle and L.W.C. Miles, The Setting of Fibers and Fabrics, Marrow Publishing Co Ltd: England, 1971.

[21] S.B. Warner, Fiber Science, Prentice-Hall, Inc: New Jersey, 1995.

[22] J.A. Brydson, Flow Properties of Polymer Melts 2ed, George Godwin Limited: London, 1981.

[23] B. Younes and A. Fotheringham, "Factorial Optimisation of the Effects of Extrusion Temperature Profile and Polymer Grade on As-spun Aliphatic-Aromatic Co-Polyester Fibers III. Mechanical Properties," *The Journal of the Textile Institute*, vol. 103, pp. 139-153, 2012.

[24] B. Younes and A. Fotheringham, "Factorial Optimisation of the Effects of Melt Spinning Conditions on Biodegradable As-Spun Aliphatic-Aromatic Co-Polyester Fibers III. Diameter, Tensile Properties and Thermal shrinkage," *Journal of Applied Polymer Science*, vol. 122, pp. 1434-1449, 2011.

[25] S.J. Kadolph and A.L. Langford, Textiles, 9th ed., Pearson Education Inc New Jersey, USA, 2002.

[26] Z. Zhang, "Application of experimental design in new product development," *The TQM Magazine*, vol. 10, pp. 432-437, 1998.

[27] W.P. Gardiner and G. Gettinby, "Experimental Design Techniques in Statistical Practice, A practical Software-Based Approach," Horwood Publishing Limited: Chichester, England, 1998.

[28] J.G. Vlachogiannis and R.K. Roy, "Robust PID controllers by taguchi method," *The TOM magazine*, vol. 17, pp. 456-466, 2005.

[29] J. Antony, D. Perry, C. Wang, and M. Kumar, "An application of taguchi method of experimental design for new product design and development process," *Assembly automation*, vol. 26, pp.18-24, 2006.

[30] "NICNAS National Industrial Chemicals Notification and Assessment Scheme," CAS Number 60961-73-1, 2003.

[31] D.W. Connell, "General Characteristics of Organic Compounds Which Exhibit Bioaccumulation," in: Bioaccumulation of Xenobiotic Compounds, CRC Press: Boca Raton, Florida, pp. 47-57, 1990.

[32] J.V. Nabholz, P. Miller, and M. Zeeman, "Environmental Risk Assessment of the New Chemicals under the Toxic Substances Control Act (TSCA) Section Five, Environmental Toxicology and Risk Assessment, ASTM STP 1179," Wayne G. Landis, Jane S. Hughes, and Michael A. Lewis ASTM: Philadelphia, 1993.

[33] U. Witt, T. Einig, M. Yamamoto, I. Kleeberg, W.-D. Deckwer, and R.-J. Müller, "Biodegradation of aliphatic–aromatic copolyesters: evaluation of the final biodegradability and ecotoxicological impact of degradation intermediates," *Chemosphere*, vol. 44, pp. 289-299, 2001.

[34] B. Younes, A. Fotheringham and H.M. EL-Dessouky, "Birefringent approach for assessing the influence of the extrusion temperature profile on the overall orientation of as-spun aliphatic-aromatic co-polyester fibers," *Polymer Engineering & Science*, vol. 49, pp. 2492-2500, 2009.

[35] B. Younes, A. Fotheringham, and H.M. EL-Dessouky, "Factorial Optimisation of the Effects of Extrusion Temperature Profile and Polymer Grade on As-spun Aliphatic-Aromatic Co-Polyester Fibers, I. Birefringence and Overall Orientation," *Journal of Applied Polymer Science*, vol. 118, pp. 1270-1277, 2010.

[36] B. Younes and A. Fotheringham, "Factorial Optimisation of the Effects of Extrusion Temperature Profile and Polymer Grade on As-spun Aliphatic-Aromatic Co-Polyester Fibers, II. Crystographic Order," *Journal of Applied Polymer Science*, vol. 119, pp. 1896-1904, 2011.

[37] B. Younes, A. Fotheringham, H.M. EL-Dessouky, and G. Haddad, "Factorial Optimisation of the Effects of Melt Spinning Conditions on As-spun Aliphatic-Aromatic Co-Polyester Fibers I. Spin Draw Ratio, Overall Orientation and Drawability," *International Journal of Polymeric Materials*, vol. 60, pp. 316-339, 2011.

DOI: 10.5963/AMSA0304003

[38] M.J. Stevens, *Extruder Principles and Operation*, Elsevier Applied Science Publishers LTD: England, UK, 1986.

[39] R.H. Lochner and J.E. Mater, *Design for Quality*, Chapman and Hall: London, 1990.

[40] M.S. Phadke, *Quality Engineering Using Robust Design*, Prentice Hall: Englewood Cliffs, New Jersey, 1989.

[41] B. Younes, A. Fotheringham, and R. Mather, "Statistical Modelling of the Effect of Multi-Stage Hot Drawing on the Thermal Shrinkage and Crystallographic Order of Biodegradable Aliphatic-Aromatic Co-Polyester Fibers," *Fibers and Polymers*, vol. 12, pp. 778-788, 2011.

[42] B. Younes, A. Fotheringham, H.M. EL-Dessouky, and G. Haddad, "A Statistical Analysis of the Influence of multi-stage hot-drawing on the overall orientation of biodegradable aliphatic-aromatic co-polyester fibers," *Journal of Engineered Fibers and Fabrics*, vol. 8, pp. 6-16, 2013.

[43] B. Younes, A. Fotheringham, and R. Mather, "Factorial Optimisation of the Effects of Melt Spinning Conditions on Biodegradable As-spun Aliphatic-Aromatic Co-Polyester Fibers II. Die head pressure, Crystallographic Order and Thermo-graphic Measurement," *International Polymer Processing*, vol. 26, iss. 2, pp. 150-163, 2011.

DOI: 10.5963/AMSA0304003